

Character Expansion, Zeros of Partition Function and θ -Term in U(1) Gauge Theory

Ahmed S. HASSAN, Masahiro IMACHI * , Norimasa TSUZUKI**
Department of Physics, Kyushu University, Fukuoka 812-81, JAPAN

Hiroshi YONEYAMA ***

Department of Physics, Saga University, Saga 840, JAPAN

Abstract

Character expansion developed in real space renormalization group (RSRG) approach is applied to U(1) lattice gauge theory with θ -term in 2 dimensions. Topological charge distribution $P(Q)$ is shown to be of Gaussian form at any β (inverse coupling constant). The partition function $Z(\theta)$ at large volume is shown to be given by the elliptic theta function. It provides the information of the zeros of partition function as an analytic function of $\zeta = e^{i\theta}$ ($\theta =$ theta parameter). These partition function zeros lead to the phase transition at $\theta = \pi$. Analytical results will be compared with the MC simulation results. In MC simulation, we adopt (i) “set method” and (ii) “trial function method”.

08/95

* e-mail:imac1scp@mbox.nc.kyushu-u.ac.jp

** e-mail:tsuz1scp@mbox.nc.kyushu-u.ac.jp

*** e-mail:yoneyama@math.ms.saga-u.ac.jp

1. Introduction

The numerical approach to the system with θ -term suffers from the difficulty, because the Boltzmann weight is complex valued and cannot be adopted as the probability weight directly. The character expansion method developed in the real space renormalization group approach is not affected by this difficulty[1][2][3][4]. It plays quite powerful role to understand the gauge systems with θ -term [5][6][7][8]. The calculation is based on the orthonormal property of the irreducible group characters. It can be performed in the system with θ -term without any difficulty.

Moreover the existence of the θ -term leads to some new features[9][10] [11] [12][13] [14][15] in the nature of partition function and leads to new physical situation[12]which are absent in the system without θ -term[16].

We present in this paper the character expansion for the U(1) gauge theory with θ -term in two dimensions. The action is assumed to be the sum of Wilson real action with real (inverse) coupling β and standard imaginary θ -term action with the coupling $\alpha = \theta/2\pi$. The expression for the partition function at any β , i.e., in both strong and weak coupling regions, will be provided and it leads to an expression for topological charge (Q) distribution ($P(Q)$) at any β .

We obtain Gaussian distribution, $P(Q) \propto \exp(-\kappa_V(\beta)Q^2)$, where $\kappa_V(\beta)$ is a constant determined by the value of real coupling constant β and the size of the volume V . The concrete expression of $\kappa_V(\beta)$ will be given. In the weak coupling regions, it can be expressed as

$$\kappa_V(\beta) = C(\beta)/V \propto \beta/V, \quad (1.1)$$

and $C(\beta)$ approaches $C_\infty \times \beta$ in $\beta \rightarrow \infty$ limit ($C_\infty \approx 19.7$). In the strong coupling limit,

$$C(0) = 6. \quad (1.2)$$

This result will be compared with numerical analysis.

Here we note about the numerical approach[17]. As mentioned above, the Boltzmann factor for the action composed of both real and imaginary parts can not be adopted as probability weight. So we use the probability weight given by the real action only and calculate the topological charge distribution $P(Q)$. Then the Fourier series of $P(Q)e^{i\theta Q}$ gives us the partition function.

The comparison of $P(Q)$ given by the character expansion method with that by numerical simulation will be given. We see quite good agreement between these approaches in all regions of the real coupling β .

In the MC approach to obtain $P(Q)$, there is a technical difficulty related to the Q dependence of $P(Q)$. The function $P(Q)$ is quite rapidly decreasing function of Q at large $|Q|$ and the numerical simulation of $P(Q)$ in large range of $|Q|$, at once is impossible. The ways to escape this difficulty are[17][18],

- (i) The MC simulation is performed in the sets of smaller $|Q|$ range. This is said “set method ”[19] and afterwards the results in these sets are gathered by adjusting neighboring results.
- (ii) Even if the range is decomposed into sets, the obtained weight $P(Q)$ still changes too rapidly in each set. So we use improved $P(Q)$. Improved $P(Q)$ is given by normalizing $P(Q)$ by appropriate trial function of $P(Q)$ which is obtained by foregoing small numerical simulation or by some theoretical prediction if we have it.

In all regions of β , the topological charge distribution is found to be expressed by Gaussian form $P(Q) \propto \exp(-\kappa_V(\beta)Q^2)$ quite well and we have an interesting analytical expression for the partition function $Z_V(\theta)$. It is expressed as the third elliptic function ϑ_3 in the large volume limit($V \rightarrow \infty$). It leads to infinite series of zeros of $Z_V(\theta)$ on real negative axis of $\zeta(\equiv e^{i\theta})$ plane, since ϑ_3 has the form of infinite product of linear function of ζ . The closest zero to the physical point $\theta = \pi(\zeta = -1)$ suggests there is a first order phase transition[20][21] at $\theta = \pi$. The distance, $\text{Im}\theta = \kappa_V(\beta)$, of this closest zero to $\zeta = -1$ is proportional to $1/V$ at any β *) and an analytical expression for this distance is given as a function of β .

*) Wiese obtained analytical estimate at $\beta = 0$.

2. Character Expansion

(2.1) Character Expansion

We will present the character expansion for the partition function of the U(1) gauge theory with θ -term. The partition function is

$$Z_V(\theta) = \int [dx_l] e^{\sum_p (-s(x_p) + iv(x_p))},$$

where x_l and x_p ($p = 1, \dots, V$) denotes the link and the plaquette variable, respectively. The action is given by the Wilson real action and standard imaginary action,

$$-s(x) + iv(x) = \beta \cos x + i\alpha x \quad (2.1)$$

where $x = F_{01}$ (F_{01} means the field strength), $\beta = 1/g^2$ and $\alpha = \theta/2\pi$. Single plaquette contribution is

$$F_p(x) = \exp\{-s(L, x) + iv(L, x)\} \quad (2.2)$$

The partition function for volume V is

$$Z_V(\theta) = \int_{-\pi}^{\pi} [dx_l] \mathcal{F}(x_1, \dots, x_V) \quad (2.3)$$

where F -function \mathcal{F} is given by

$$\mathcal{F}(x_1, \dots, x_V) = \sum_{Q=-\infty}^{\infty} F(x_1, \dots, x_V) \delta(x_1 + \dots + x_V - 2\pi Q). \quad (2.4)$$

In (2.4), Q denotes the topological charge (integer). By use of Poisson sum formula, \mathcal{F} can be written as

$$\mathcal{F}(x_1, \dots, x_V) = \sum_{l=-\infty}^{\infty} F(x_1, \dots, x_V) e^{il(x_1 + \dots + x_V)} \quad (2.5)$$

The functional $F(x_1, \dots, x_V)$ is a product of plaquette contributions,

$$F(x_1, \dots, x_V) = F_p(x_1) F_p(x_2) \dots F_p(x_V) \quad (2.6)$$

The character expansion for F_p is

$$F_p(x) = \sum_{m=-\infty}^{\infty} \tilde{F}_m(\beta, \alpha) \chi_m(x), \quad (2.7)$$

$$\chi_m(x) = \exp(imx), m = \text{integer},$$

where $\chi_m(x)$ denotes the irreducible character specified by integer m . Then

$$\begin{aligned}
\mathcal{F}(x_1, \dots, x_V) &= \sum_{l=-\infty}^{\infty} F_p(x_1)F_p(x_2)\dots F_p(x_V)e^{il(x_1+\dots+x_V)} \\
&= \sum_{l=-\infty}^{\infty} \prod_{k=1}^V \sum_{m_k} \tilde{F}_{m_k}(\beta, \alpha)\chi_{m_k}(x_k)\chi_l(x_k) \\
&= \sum_{l=-\infty}^{\infty} \prod_{k=1}^V \sum_{m_k} \tilde{F}_{m_k}(\beta, \alpha)\chi_{m_k+l}(x_k) \\
&= \sum_{l=-\infty}^{\infty} \prod_{k=1}^V \sum_{m_k} \tilde{F}_{m_k-l}(\beta, \alpha)\chi_{m_k}(x_k)
\end{aligned} \tag{2.8}$$

The character expansion coefficient is[5]

$$\tilde{F}_m(\beta, \alpha) = \sum_n \tilde{F}_n^s(\beta)\tilde{F}_{m-n}^v(\alpha), \tag{2.9}$$

where character expansion of $\exp(-s)$ and $\exp(iv)(= \exp(-i\alpha x))$ are respectively,

$$\begin{aligned}
\tilde{F}_n^s(\beta) &= I_n(\beta), \\
\tilde{F}_l^v(\alpha) &= \frac{\sin \pi(\alpha + l)}{\pi(\alpha + l)},
\end{aligned} \tag{2.10}$$

where $I_n(\beta)$ denotes the modified Bessel function. It satisfies the relation

$$\tilde{F}_{m+l}(\beta, \alpha) = \tilde{F}_m(\beta, \alpha + l) \tag{2.11}$$

Then

$$\mathcal{F}(x_1, \dots, x_V) = \sum_{l=-\infty}^{\infty} \prod_{k=1}^V \sum_{m_k} \tilde{F}_{m_k}(\beta, \alpha - l)\chi_{m_k}(x_k) \tag{2.12}$$

Now we integrate all the inner links except for the outermost link variables.

$$\begin{aligned}
\int_{-\pi}^{\pi} \prod_l dx_{l=\text{innerlink}} \mathcal{F}(x_1, \dots, x_V) &= \sum_l \sum_m \tilde{F}_m(\beta, \alpha - l)^V \chi_m(x_1 + \dots + x_V) \\
& \quad y = x_1 + \dots + x_V = \text{outermost link variable.}
\end{aligned} \tag{2.13}$$

where the orthogonality

$$\int_{-\pi}^{\pi} \frac{dv}{2\pi} \chi_{m_1}(x_1 + v)\chi_{m_2}(x_2 - v) = \delta_{m_1 m_2} \chi_{m_1}(x_1 + x_2) \tag{2.14}$$

is repeatedly used. The partition function is

$$\begin{aligned}
Z_V(\theta) &= \int_{-\pi}^{\pi} \frac{dy}{2\pi} \sum_l \sum_m \tilde{F}_m(\beta, \alpha - l)^V \chi_m(y) \\
&= \sum_l \sum_m (\tilde{F}_m(\beta, \alpha - l))^V \delta_{m,0} \\
&= \sum_l (\tilde{F}_0(\beta, \alpha - l))^V,
\end{aligned} \tag{2.15}$$

where

$$\tilde{F}_0(\beta, \alpha - l) = \sum_{n=-\infty}^{\infty} I_n(\beta) \frac{\sin \pi(\alpha + l - n)}{\pi(\alpha + l - n)}. \tag{2.16}$$

(2.2) Topological charge distribution

Topological charge distribution appears in

$$Z_V(\theta) = \sum_{Q=-\infty}^{\infty} P(Q) e^{i\theta Q}, \tag{2.17}$$

and $P(Q)$ is

$$P(Q) = \int_{-1/2}^{1/2} d\alpha Z_V(\theta) e^{-i2\pi\alpha Q}. \tag{2.18}$$

Eqs.(2.15) and (2.17) lead to,

$$\begin{aligned}
P(Q) &= \int_{-1/2}^{1/2} d\alpha \sum_{l=-\infty}^{\infty} (\tilde{F}_0(\beta, \alpha - l))^V e^{-i2\pi\alpha Q} \\
&= \int_{-\infty}^{\infty} d\alpha (\tilde{F}_0(\beta, \alpha))^V e^{-i2\pi\alpha Q},
\end{aligned} \tag{2.19}$$

where $\tilde{F}_0(\beta, \alpha)$ is given by eq.(2.16) setting $l = 0$. This is an exact expression in β .

We will evaluate (2.19) in large V limit. The character coefficient $\tilde{F}_0(\beta, \alpha)$ is an even function of α and peaked at $\alpha = 0$. In large V limit, $(\tilde{F}_0(\beta, \alpha))^V$ is a function sharply peaked at $\alpha = 0$. So we can evaluate its contribution by the Taylor expansion around $\alpha = 0$.

$$\begin{aligned}
\tilde{F}_0(\beta, \alpha) &= \sum_{n=-\infty}^{\infty} I_n(\beta) \frac{\sin \pi(\alpha + n)}{\pi(\alpha + n)} \\
&= I_0(\beta) \frac{\sin \pi\alpha}{\pi\alpha} + 2 \sum_{n=1}^{\infty} I_n(\beta) \frac{\sin \pi(\alpha + n)}{\pi(\alpha + n)} \\
&= I_0(\beta) \left(1 - \frac{\pi^2}{6} \alpha^2\right) - 2\alpha^2 \sum_{n=1}^{\infty} I_n(\beta) \frac{(-1)^n}{n^2} + O(\alpha^4) \\
&\cong I_0(\beta) \left[1 - \left(\frac{\pi^2}{6} + \frac{2}{I_0(\beta)} \sum_{n=1}^{\infty} I_n(\beta) \frac{(-1)^n}{n^2}\right) \alpha^2\right] \\
&\cong I_0(\beta) \exp(-G(\beta)\alpha^2),
\end{aligned} \tag{2.20}$$

with

$$G(\beta) = \frac{\pi^2}{6} + \frac{2}{I_0(\beta)} \sum_{n=1}^{\infty} I_n(\beta) \frac{(-1)^n}{n^2}, \quad (2.21)$$

for any β .

Now we have

$$\begin{aligned} P(Q) &= 2 \int_0^{\infty} d\alpha \exp(-G(\beta)V\alpha^2) \cos(2\pi\alpha Q) \\ &= \sqrt{\frac{\pi}{GV}} \exp\left(\frac{-\pi^2}{G(\beta)V} Q^2\right) \\ &= \sqrt{\frac{\pi}{GV}} \exp(-\kappa_V(\beta)Q^2). \end{aligned} \quad (2.22)$$

The quantity $\kappa_V(\beta)$ is defined by

$$\kappa_V(\beta) = \frac{\pi^2}{G(\beta)V}. \quad (2.23)$$

We define

$$C(\beta) = \kappa_V(\beta)V = \frac{\pi^2}{G(\beta)}. \quad (2.24)$$

Topological charge distribution has the Gaussian form. The coefficient $\kappa_V(\beta)$ has the “ $1/V$ ” form for all β . The coefficient $C(\beta)$ is plotted as a function of β in Fig.1.

Fig. 1

It is given, in the strong coupling limit, by

$$\begin{aligned} G(0) &= \frac{\pi^2}{6}, \\ C(0) &= 6. \end{aligned} \quad (2.25)$$

In weak coupling regions ($\beta \gtrsim 1$), it seems proportional to β . The value of $C(\beta)/\beta$, however, changes slightly with β (Fig.2).

Fig. 2

(2.3) Partition function zeros and phase transition

When $P(Q)$ is given by Gaussian form (2.22), the partition function

$$Z_V(\theta) = \sum_Q P(Q) e^{2\pi i \alpha Q} = \sum_{Q=-\infty}^{\infty} P(Q) \zeta^Q, \quad (2.26)$$

has a simple factorized form ^{*)}

$$\begin{aligned}
Z_V(Q) &= \sqrt{\frac{\pi}{GV}} \sum_Q \exp(-\kappa_V(\beta)Q^2) e^{2\pi i\alpha Q}, \\
&= \sqrt{\frac{\pi}{GV}} q_0 \prod_{n=1}^{\infty} (1 + q^{2n-1}\zeta) \left(1 + \frac{q^{2n-1}}{\zeta}\right),
\end{aligned} \tag{2.27}$$

where $\zeta \equiv e^{i\theta} = e^{2\pi i\alpha}$ and

$$\begin{aligned}
q_0 &= \prod_{n=1}^{\infty} (1 - q^{2n}), \\
q &= \exp(-\kappa_V(\beta)), \quad (< 1).
\end{aligned} \tag{2.28}$$

It can be written as

$$Z_V(\theta) = \sqrt{\frac{\pi}{GV}} \vartheta_3(\nu, \tau), \tag{2.29}$$

where $\vartheta_3(\nu, \tau)$ is the third elliptic theta function with $q = \exp(i\pi\tau)$ and $\alpha = \nu$.

Important feature of (2.27) is that the partition function has infinite zeros (at $V \rightarrow \infty$) on the real negative ζ axis in complex ζ plane. It shows that the system undergoes transition at $\theta = \pi$. When V is finite, the closest zero of $Z_V(\theta)$ to $\zeta = -1$ ($\theta = \pi$) is located at the distance $\text{Im}\theta = \kappa_V(\beta) \propto 1/V$ from $\zeta = -1$ point. In $V \rightarrow \infty$ limit, it approaches the $\zeta = -1$ point and infinitely many zeros accumulate on the real negative axis of complex ζ plane.

Poisson sum formula applied to (2.17) gives

$$\begin{aligned}
&\sum_Q \exp(-\kappa_V Q^2 + 2\pi i\alpha Q) \\
&= \sum_m \int_{-\infty}^{\infty} d\xi \exp(-\kappa_V \xi^2 + 2\pi i\alpha \xi + 2\pi i\xi m) \\
&= \sqrt{\frac{\pi}{\kappa_V}} \sum_m \exp\left(-\frac{\pi^2}{\kappa_V} (\alpha - m)^2\right).
\end{aligned} \tag{2.30}$$

Note that this is a periodic Gaussian form and that it shows clearly the phase structure as follows; For $m_0 - 1/2 < \alpha < m_0 + 1/2$, the sum is dominated by $m = m_0$ and for $m_0 + 1/2 < \alpha < m_0 + 3/2$ the sum is dominated by $m = m_0 + 1$. It shows that there are infinitely many phase transitions at $\alpha = m_0 + 1/2$, i.e., at $\theta = \pi + 2\pi m_0$ ($m_0 = \text{any integer}$).

Eq. (2.30) can also be written as,

^{*)} The authors are grateful to Prof. Y. Yamada for valuable discussion on this point.

$$\sqrt{\frac{\pi}{\kappa_V}} \exp\left(-\frac{\pi^2 \alpha^2}{\kappa_V}\right) \sum_m \exp\left(-\frac{\pi^2}{\kappa_V} m^2 - \frac{2\pi^2 \alpha^2}{\kappa_V} m\right). \quad (2.31)$$

The left hand side of (2.30) is $\vartheta_3(\nu, \tau)$. Eq.(2.31) is just the same form as the left hand side of (2.30) if we replace $\kappa_V \rightarrow \kappa'_V = \pi^2/\kappa_V$, $\alpha \rightarrow \alpha' = i\alpha\pi/\kappa_V$. Then we have

$$\vartheta_3(\nu, \tau) = \sqrt{\frac{1}{i\tau}} \exp\left(\frac{i\pi\nu^2}{\tau}\right) \vartheta_3(\nu', \tau') \quad (2.32)$$

where

$$\begin{aligned} \nu &= \alpha, \\ i\pi\tau &= -\kappa_V, \\ \tau' &= -1/\tau, \\ \nu' &= \nu/\tau. \end{aligned} \quad (2.33)$$

Eq (2.33) is a kind of modular transformation.

3. Comparison with numerical method

When we adopt the action with θ -term, the Boltzmann factor

$$\exp(-s(x) + iv(x))$$

is a complex number and cannot be directly used as a probability weight. The partition function can be written

$$\begin{aligned} Z_V(\theta) &= \int [dx_l] \exp\left(-\sum_p s(x_p) + i\alpha \sum_p x_p\right) \\ &= \sum_Q \int [dx_l]^{(Q)} \exp\left(-\sum_p s(x_p)\right) e^{2\pi i\alpha Q} \\ &= \sum_Q P(Q) e^{2\pi i\alpha Q} \end{aligned} \quad (3.1)$$

where $[dx_l]^{(Q)}$ is the integration measure restricted to topological charge Q . We first calculate the topological charge distribution $P(Q)$ with real positive probability weight $\exp(-\sum s(x_p))$ and then we obtain $Z_V(\theta)$ through Fourier series. In order to perform numerical simulations to obtain $P(Q)$, a technical problem appears because $P(Q)$ is usually a quite rapidly decreasing function of Q and it drops by many decades at large Q . Two technical methods to avoid this difficulty will be used.

- (i) “Set method”: Wide range of Q is divided into many sets. Each set composed of $[Q, Q + 1, \dots, Q + s - 1]$. In the actual calculation we choose $s = 4$. Neighboring sets are adjusted at the overlapping Q so as to give $P(Q)$ over these neighboring sets with the common normalization. Consider two neighboring sets $[Q - (s - 1), \dots, Q]$ and $[Q, Q + 1, \dots, Q + s - 1]$. We equate the value of $P(Q)$ at largest $Q(= Q)$ of the lower set with that at the smallest $Q(= Q)$ of the upper set.
- (ii) “Trial function method (Improved $P(Q)$)”: Even we divide into sets, the change of $P(Q)$ in each set is still large. We define improved $\bar{P}(Q)$ dividing $P(Q)$ by trial $P_t(Q)$, “ $P_t(Q)$ ”

$$\bar{P}(Q) = P(Q)/P_t(Q). \quad (3.2)$$

Eq.(3.2) will give very slowly changing or almost flat distribution if we use appropriate trial distribution $P_t(Q)$. We perform Monte Carlo simulation for U(1) gauge theory at $\beta = 0.0$ (strong coupling limit), 1.0, 2.0, 3.0, 4.0 and 5.0 (weak coupling regions), at volume $V = 100$ and 400.

Table I

β	$C(\beta)$	$C(\beta)/\beta$	measured $C(\beta)$	
			$V=100$	$V=400$
0	6	∞	5.99	5.53
0.5	8.410	16.79		
1.0	12.30	12.30	12.4	12.0
1.2	14.38	11.98		
2.0	25.82	12.91	24.4	25.8
2.4	33.13	13.80		
3.0	45.20	15.07	40.5	45.1
4.0	66.19	16.55	57.8	66.3
5.0	86.87	17.37		85.7
10.0	186.8	18.68		
15.0	285.8	19.05		
20.0	384.6	19.23		
100.0	1960	19.60		

Measurements are made 10^4 times for each set. Measured range of Q are from 0 to $Q_{\text{Max}} = 15$ and from 0 to 30 for $V = 100$ ($=10 \times 10$) and 400 ($=20 \times 20$), respectively.

$P(Q)$ changes by $O(10^{-56})$ for $\beta = 4.0$ at $V = 100$ and by $O(10^{-82})$ for $\beta = 5.0$ at $V=400$ between $Q = 0$ and $Q = Q_{\text{Max}}$.

The distributions obtained through MC simulation show Gaussian distribution of Q for all the cases. They are shown in fig.3(a) and (b).

Fig. 3(a)

Fig. 3(b)

The data for $P(Q)$ is taken by the histogram method and the multinomial distribution is assumed to obtain statistical error in each set. The obtained error is $\approx 2\%$ of the measured $P(Q)$ and much smaller than the symbol of data points in the figure.

The slope $\kappa_V(\beta)$ of Q^2 in the Gaussian form coincides quite well with the analytical prediction of eq (2.23). The slope parameter $\kappa_V(\beta)$ obtained by numerical calculations shows $1/V$ law for each β and the value $C(\beta) \equiv \kappa_V(\beta)V$ (eq.(2.23) and (2.24)) is almost V -independent(Table (I)). The fact that all the $P(Q)$'s measured for $\beta= 1.0, 2.0, 3.0, 4.0$ and 5.0 have the Gaussian distribution shows that the system undergoes the first order phase transition at $\theta = \pi$ for all these β values.

4. Conclusions

We presented the analytic form of partition function $Z(\theta)$ for U(1) lattice gauge theory with θ -term in 2 dimensions. Character expansion of RSRG can be safely applied to the system with θ -term. In character expansion method, only orthonormal property of irreducible characters is used and the problem of complex Boltzmann factor is harmless in this approach. Topological charge distribution for any real coupling constant β is given analytically, and is shown to have Gaussian form. The coefficient $\kappa_V(\beta)$ in Gaussian form is analytically given. This form of $P(Q)$ leads to $Z(\theta)$ expressed by the elliptic theta function ϑ_3 in $V \rightarrow \infty$ limit. This function is known to have infinite numbers of zeros on the real negative axis of $\zeta = e^{i\theta}$. The closest zero to -1 provides the information about the deconfining phase transition at $\theta = \pi$. The distance from $\zeta = -1$ is $\text{Im}\theta = \kappa_V(\beta) \propto 1/V$ indicates that the phase transition is consistent with the first order one[20][21].

The results for $P(Q)$ given above at any β is compared with the numerical simulations. In numerical simulations the famous problem of complex Boltzmann factor appears. The numerical results thus obtained agree with the analytical results quite well. Topological charge distribution $P(Q)$ obtained by numerical simulations obeys Gaussian form. The coefficient $\kappa_V(\beta)$ of Q^2 in the exponent of the Gaussian is proportional to $1/V$. We covered a wide range in both of Q (up to $Q_{\text{Max}} = 30$) and $P(Q)$ (changes by order 10^{-82}). We comment here on numerical simulations of $P(Q)$ of CP^1 model [18]in two dimensions. The

results of the model at strong couplings also show Gaussian form, and the coefficient obeys $1/V$ law.

Poisson sum formula leads to an interesting expression eq.(2.30) for the partition function. It is given by periodic Gaussian form. Since $1/\kappa_V \propto V \rightarrow$ large, this expression shows phase transition clearly. For $m_0 - 1/2 < \alpha < m_0 + 1/2$ (i.e. $m_0 - \pi < \theta < m_0 + \pi$), $m = m_0$ dominates due to large coefficient in front of $(m - \alpha)^2$. For $m_0 + 1/2 < \alpha < m_0 + 3/2$ ($\pi + 2\pi m_0 < \theta < 3\pi + 2\pi m_0$), $m = m_0 + 1$ dominates. From this argument we understand the critical value $\alpha_c = m_0 + 1/2$ ($m_0 =$ any integer). Poisson sum formula also relates $\vartheta_3(\nu, \theta)$ to a modular transformed form $\vartheta_3(\nu', \theta')$ (2.32 and (2.33)).

References

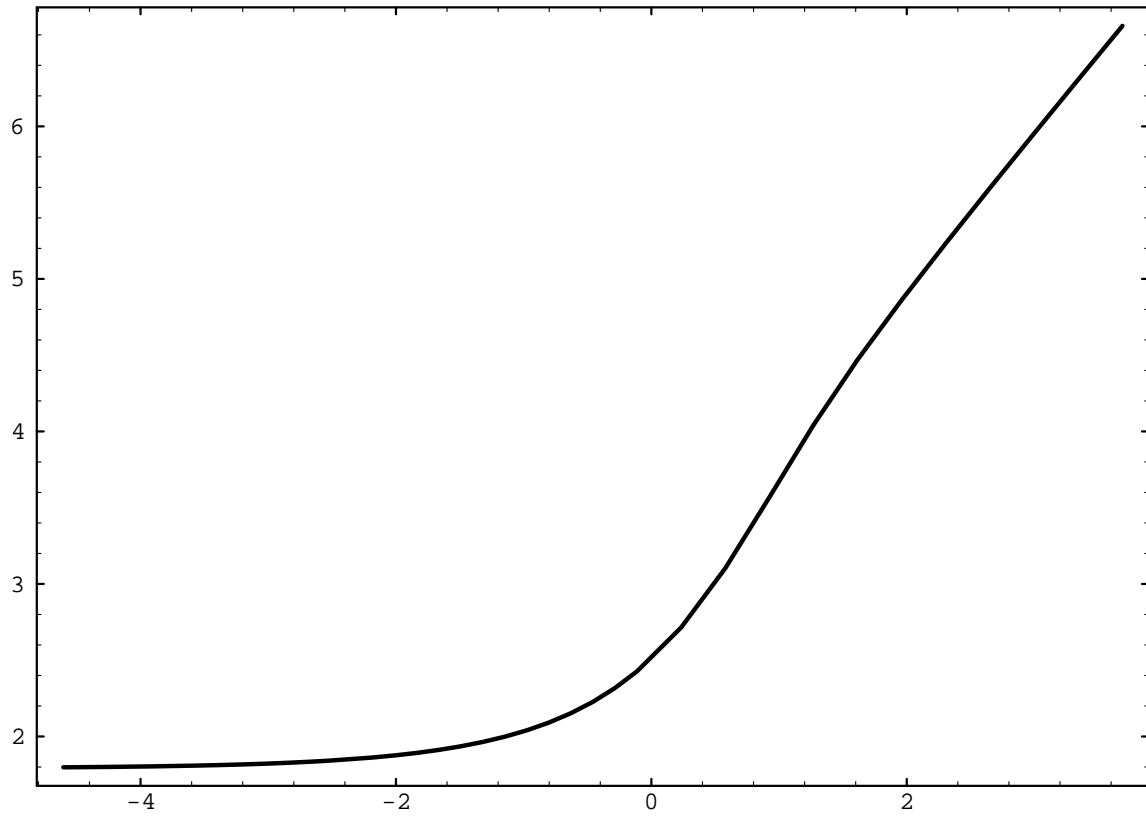
- [1] A. A. Migdal, Sov. Phys. JETP **42**(1976)413, 743.
- [2] L. P. Kadanoff, Ann. Phys. **100**(1976)359.
- [3] K. M. Bitar, S. Gottlieb and C. K. Zachos, Phys. Rev. **26**(1982)2853, Phys. Lett. **B121**(1983)163.
- [4] M. Imachi, S. Kawabe and H. Yoneyama, Prog. Theor. Phys. **69**(1983) 221, 1005.
- [5] A. S. Hassan, M. Imachi and H. Yoneyama, Prog. Theor. Phys. **93**(1995) 161.
- [6] T. G. Kovacs and J. F. Wheeler, Mod. Phys. Lett. **A6**(1991)2827.
- [7] T. G. Kovacs, E. T. Tomboulis and Z. Schram preprint UCLA/95/TEP/14, hep-th/9505005.
- [8] M. Asorey, J. G. Esteve and J. Salas, J. Phys.**A** **27**(1994)3707.
- [9] G. 't Hooft, Nucl. Phys. **B190**[FS3](1981)455.
- [10] J. L. Cardy and E. Rabinovici, Nucl. Phys. **B205**[FS5](1982)1.
- [11] J. L. Cardy, Nucl. Phys. **B205**[FS5](1982)17.
- [12] E. Fradkin and F. A. Shaposnik, Phys. Rev. Lett. **66** (1991)267.
- [13] S. Coleman, Ann. Phys. **101**(1976)239.
- [14] G. Schierholz, “ θ Vacua, Confinement and The Continuum Limit”, preprint DESY 94-229, HLRZ 94-63.
- [15] G. Schierholz, hep-lat/9409019.
- [16] A. M. Polyakov, Nucl. Phys. **B120**(1977) 429.
- [17] U. -J. Wiese, Nucl. Phys. **B318**(1989)153.
- [18] A. S. Hassan, M. Imachi, N. Tsuzuki and H. Yoneyama, “Topological charge distribution and CP^1 model with θ -term, Kyushu-HET-26, SAGA-HE-91(Aug. 1995).”
- [19] G. Bhanot, S. Black, P. Carter and R. Salvador, Phys. Lett. **B183**(1987) 331.
- [20] M. E. Fisher and A. N. Berker, Phys. Rev. **B** **26**,(1982) 2507 .
- [21] C. Itzykson, R. B. Pearson and J. B. Zuber, Nucl. Phys. **B** **220**[FS8] (1983),415.

TABLE CAPTIONS

Table I Coefficients in Gaussian distributions are shown for β at 0, 0.5, 1.0, \dots 100.

FIGURE CAPTIONS

- Fig. 1 $\ln[C(\beta)]$ vs. $\ln[\beta]$. $C(\beta)$ is approximately linear function of β in weak coupling regions.
- Fig. 2 $C(\beta)/\beta$ vs. β . We can see approximately constant behavior at large β .
- Fig. 3(a) Topological charge distribution $\log_{10}(P(Q))$ vs. Q^2 measured by Monte Carlo simulations for various β 's. The value of Q ranges from 0 to 15($=Q_{\text{Max}}$) and the lattice size $L \times L$ is 10×10 . The inverse coupling constant β are taken to be 0.0(square), 1.0(diamond), 2.0(circle), 3.0(triangle), 4.0(cross). The lines show fittings according to the Gaussian form.
- Fig. 3(b) Topological charge distribution $\log_{10}(P(Q))$. Notations are as in Fig. 3(a). $Q_{\text{Max}}=30$ and $L = 20$. Data for $\beta = 5.0$ (nabla) is added.



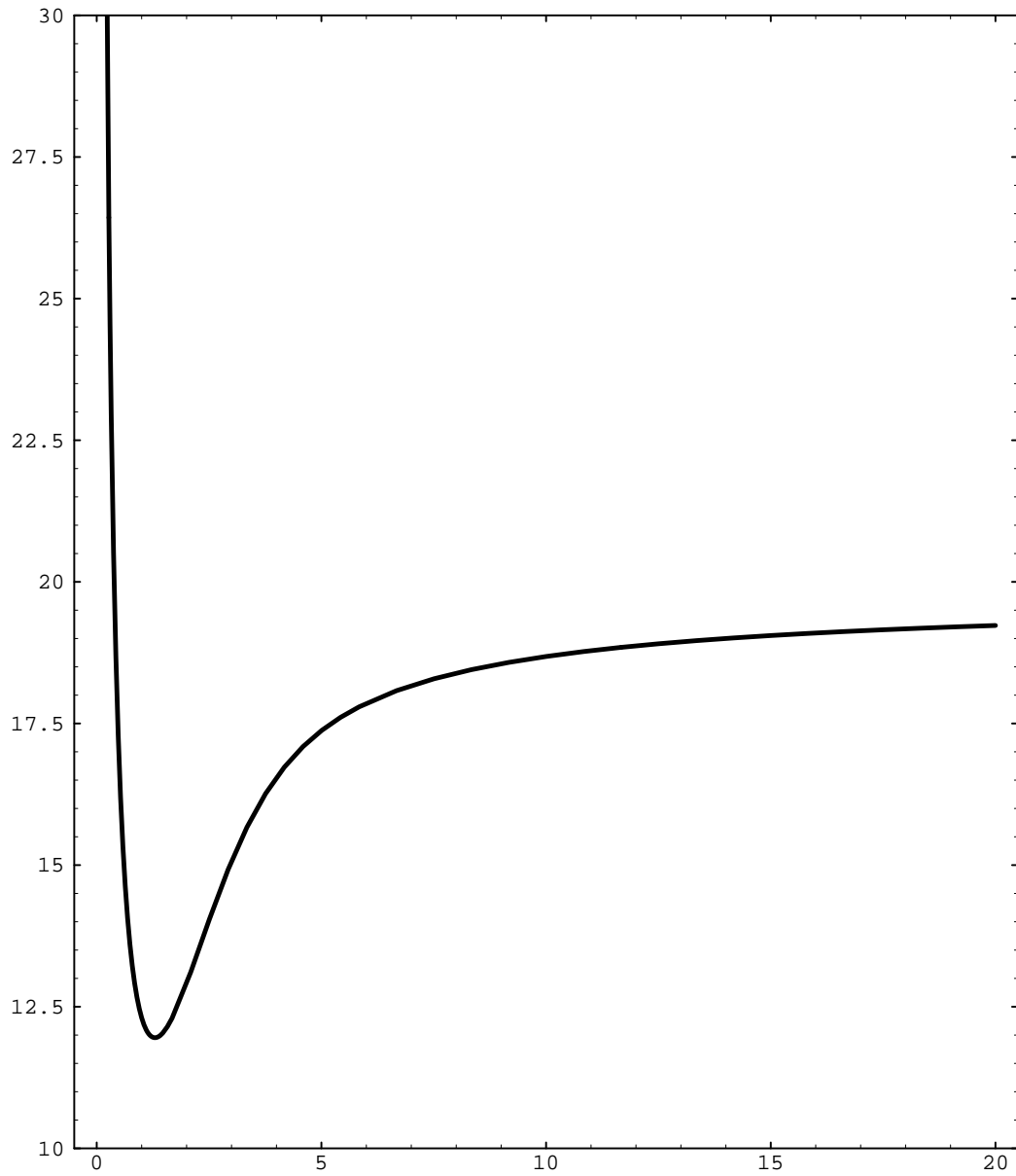


Fig. 2

